AGU PUBLICATIONS

JGR

Journal of Geophysical Research: Oceans

RESEARCH ARTICLE

10.1002/2014JC010153

Interannual variability of wintertime temperature on the inner continental shelf of the Middle Atlantic Bight

Thomas P. Connolly[1] and Steven J. Lentz[1]

[1]Department of Physical Oceanography, Woods Hole Oceanographic Institution, Woods Hole, Massachusetts, USA

Key Points:
- Broad-scale correlation of wintertime temperature anomalies at shallow locations
- Rapid time scale of adjustment toward air temperature over inner shelf
- Along-shelf advection over distances ~100 km influences air-sea heat flux

Correspondence to:
T. P. Connolly,
tconnolly@whoi.edu

Citation:
Connolly, T. P., and S. J. Lentz (2014), Interannual variability of wintertime temperature on the inner continental shelf of the Middle Atlantic Bight, *J. Geophys. Res. Oceans*, *119*, 6269–6285, doi:10.1002/2014JC010153.

Received 14 MAY 2014
Accepted 27 AUG 2014
Accepted article online 30 AUG 2014
Published online 17 SEP 2014

Abstract The shallow depth of the inner continental shelf allows for rapid adjustment of the ocean to air-sea exchange of heat and momentum compared with offshore locations. Observations during 2001–2013 are used to evaluate the contributions of air-sea heat flux and oceanic advection to interannual variability of inner-shelf temperature in the Middle Atlantic Bight. Wintertime processes are important for interpreting regional interannual variability at nearshore locations since winter anomalies account for 69–77% of the variance of the annual anomalies and are correlated over broad along-shelf scales, from New England to North Carolina. At the Martha's Vineyard Coastal Observatory on the 12 m isobath, a heat budget is used to test the hypothesis that interannual differences in winter temperatures are due solely to air-sea heat flux. Bimonthly averages of air-sea heat flux are correlated with temporal changes in temperature, but overestimate the observed wintertime cooling. Velocity and satellite-derived temperature data show that interannual variability in wintertime surface cooling is partially compensated for by alongshore advection of warmer water from the west at this particular location. It is also shown that surface heat flux is a strong function of air-sea temperature difference. Because of this coupling between ocean and air temperatures in shallow water, along-shelf advection can significantly modify the surface heat flux at seasonal and interannual time scales. While along-shelf advection at relatively small (~100 km) scales can be an important component of the heat budget over the inner shelf, interannual temperature variability is still largely determined by adjustment to large-scale air-temperature anomalies.

1. Introduction

At coastal locations, diagnosing the variability of ocean temperature at interannual time scales is an important step in understanding how climate processes influence marine ecosystems. In the Middle Atlantic Bight (MAB), which extends from Cape Hatteras to Cape Cod (Figure 1a), interannual variability in ocean temperature affects the distribution of commercially important species such as lobster, surfclams, and mackeral [*Taylor et al*., 1957; *Murawski*, 1993; *Weinberg*, 2005; *Overholtz et al*., 2011], as well as parasites that affect oyster populations [*Cook et al*., 1998]. At estuarine and nearshore locations in the MAB, warm wintertime temperatures have been linked to reduced phytoplankton biomass and increased zooplankton abundance during the winter-spring bloom [*Keller et al*., 1999, 2001].

Temporal variability of temperature over the MAB continental shelf is characterized by a seasonal cycle with range 10–25°C, and smaller interannual anomalies <3°C when the seasonal cycle is removed [*Mountain*, 2003; *Shearman and Lentz*, 2010]. The interannual anomalies are significantly correlated over large along-shelf scales throughout the MAB and Gulf of Maine (GOM), and at different locations across the shelf [*Shearman and Lentz*, 2010]. At longer decadal time scales, a long-term warming trend is evident, particularly since the mid-1960s [*Nixon et al*., 2004; *Shearman and Lentz*, 2010]. Warming trends in ocean temperature over the shelf are greater than local trends in air temperature, likely due to along-shelf advection of remote temperature anomalies from farther north [*Shearman and Lentz*, 2010].

Previous studies of interannual temperature variability over the MAB shelf place different emphasis on the relative roles of oceanic advection versus air-sea exchange. Interannual temperature anomalies in the primary shelf water mass are correlated with local air temperature anomalies, suggesting that air-sea flux is the dominant factor [*Mountain*, 2003]. *Thompson et al*. [1988] show that the spatial patterns associated with interannual variability of sea surface temperature are consistent with the changes in the offshore winds that advect cold, dry air over the ocean. Similarly, *Chen et al*. [2014] attribute anomalously warm ocean

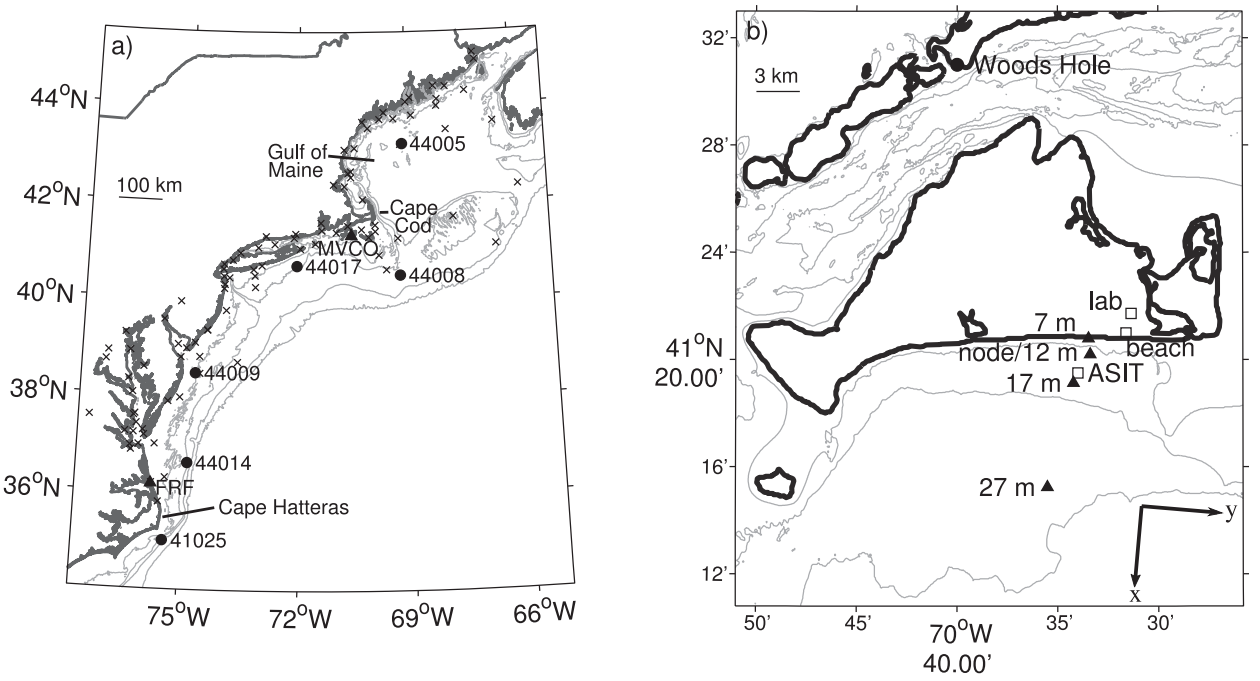

Figure 1. Locations of observations. (a) Map of the MAB, with locations of NDBC buoys (circles), SST data from *Shearman and Lentz* [2010] (crosses), and the FRF pier and MVCO (triangles). The 30, 50, 100, and 1000 m isobaths are contoured in gray. (b) Close-in map of the MVCO site on the southern continental shelf of New England, with locations of SWWIM mooring sites (triangles), wind and meteorological observations (squares), and Woods Hole SST (circle). The MVCO node is colocated at the 12 m mooring site. The coordinate system used at the node is shown in the bottom right. Isobaths are contoured at 10 m intervals.

temperatures during late fall and early winter of 2012 to reduced wintertime heat loss to the atmosphere associated with warm, moist air, and weak wind stress. In contrast, *Lee and Lwiza* [2005] show only a weak correlation between local surface heat flux and ocean temperature changes at interannual time scales in Long Island Sound, and suggest a connection to larger-scale oceanic variability at the shelf break and farther offshore.

On the inner shelf, where the surface and bottom boundary layers interact and turbulent stresses fill the entire water column, shallow water depths allow for rapid adjustment of the ocean to air-sea exchange of heat and momentum compared with offshore locations. Heat budget analyses over the inner shelf have focused primarily on the seasonal cycle, emphasizing the importance of air-sea exchange during winter and the additional contribution of cross-shelf exchange during stratified periods [*Austin*, 1999; *Fewings and Lentz*, 2011]. Off North Carolina, along-shelf advection cools the inner shelf during winter, but this cooling is relatively minor compared to the loss of heat due to air-sea exchange [*Austin*, 1999]. Off Martha's Vineyard, *Fewings and Lentz* [2011] inferred a minor role of along-shelf advection during winter due to closure of the heat budget without advection during the season studied. At both of these locations, cross-shelf exchange is thought to be a minor factor during winter when vertical temperature gradients are weak. The important processes contributing to the heat budget over the inner shelf have not yet been evaluated on interannual time scales.

This study focuses on interannual variability of wintertime temperature over the inner shelf in the MAB. The winter season is particularly important because atmospheric climate variability on interannual and decadal time scales is greater during winter months than summer months in this region [*Joyce*, 2002]. It is hypothesized that changes in temperature over the course of different winters are due solely to air-sea exchange of heat. The observations and analysis methods used to test this hypothesis are described in section 2. In section 3.1, it is shown that interannual ocean temperature anomalies throughout the MAB are particularly well correlated in the relatively shallow water of the inner shelf and that winter anomalies explain a large portion of the variance of the annual temperature anomalies. In addition, it is shown that winter temperature anomalies are correlated with local air temperature anomalies. In sections 3.2 and 3.3, air-sea heat flux and oceanic advection are quantified over multiple winter seasons over the inner shelf of Martha's Vineyard in order to test the hypothesis that interannual temperature variability over the inner shelf is primarily

associated with air-sea exchange. It is shown that along-shelf advection is an important part of the heat budget, in addition to surface heat flux.

2. Methods

2.1. Observations

2.1.1. In Situ Measurements of Sea Surface Temperature

Sea surface temperature (SST) data during the period 1984–2013 are obtained at locations throughout the MAB from the National Data Buoy Center (NDBC, http://www.ndbc.noaa.gov) and at Duck, NC from Army Corps of Engineers Field Research Facility (FRF, http://www.frf.usace.army.mil). Locations are shown in Figure 1a. Historical data from the NDBC buoys are available at 1 h intervals. Start dates for the available buoy data range from 1978 (buoy 44005) to 2003 (buoy 41025). The FRF data are from near-daily CTD casts from the end of the pier at 7 m water depth made since 1984. Measurements of air temperature from the FRF pier are also used in the analysis. In addition, monthly values of the historical SST data presented in *Shearman and Lentz* [2010] are used from locations north of Cape Hatteras during the period 1873–2007 (Figure 1a).

2.1.2. Martha's Vineyard Coastal Observatory (2001–2013)

At the Martha's Vineyard Coastal Observatory (MVCO, http://www.whoi.edu/mvco) on the southern New England shelf (Figure 1b), measurements of temperature, salinity, and velocity have been collected since June 2001 at a subsurface cabled node in 12 m water depth. Temperature and salinity data are collected 1.5 m above the bottom. Water-column velocity data are collected using an upward-looking 1200 kHz Acoustic Doppler Current Profiler (ADCP) at a rate of 2 Hz and averaged into 20 min ensembles. Bins used for analysis have 0.5 m vertical spacing at depths 2–9.5 m. To remove tidal and other high-frequency variability, velocity data are low-pass filtered using the PL64 filter with 38 h half-power point [*Rosenfeld*, 1983]. Depth-averaged velocities are computed by extending measurements in the shallowest and deepest ADCP bins to the surface and bottom, integrating the velocity profiles using a trapezoidal rule, and dividing by the water depth. The coordinate system is arranged so that the along-shelf direction (y axis) is aligned with the major axis of the principal ellipse of the depth-averaged, low-pass filtered velocity (Figure 1b). Surface wave characteristics and wave spectra measured by the ADCP are used to compute theoretical profiles of Stokes drift, which can significantly affect the cross-shelf transport of heat over the shallow inner shelf [*Fewings and Lentz*, 2011].

Meteorological observations at MVCO come from three sites: at the beach, a nearby shore laboratory, and the air-sea interaction tower (ASIT) located at the 17 m isobath (Figure 1b). Wind data from over the water at ASIT are most representative of the inner-shelf forcing, but are only available during the period August 2004 to August 2011. For the calculation of wind stress and surface heat flux at times when wind data are unavailable at ASIT, empirically adjusted data are first used from the beach, then the shore laboratory. A separate regression is used for each direction at 1° intervals to make the beach and shore laboratory data consistent with ASIT. The ASIT data account for 90–94% of variance in the eastward and northward components of wind velocity at the two other sites (not shown). Wind stress is calculated from wind velocity at the tower height of 18.4 m using the coefficients of *Smith* [1988]. The 20 min wind data are rotated to be consistent with the principle axis coordinate system of ocean velocity observed at the node.

2.1.3. Stratification, Wind, and Waves on the Inner Shelf of Martha's Vineyard (2006–2010)

The Stratification, Wind, and Waves on the Inner shelf of Martha's Vineyard (SWWIM) field program included a cross-shelf mooring array with sites at the 7, 12, 17.5, and 27.5 m isobaths (Figure 1b, see also *Ganju et al.* [2011]; *Horwitz and Lentz* [2014]). Data from the 7 and 12 m sites are used for this study. At the 7 m site, a 1200 kHz ADCP collected data at 1 Hz in 6.7 min or 9 min bursts every 20 min. Bins used for analysis have 0.25 m vertical spacing at heights 1.75 m from the bottom to within 0.75 m from the surface. Temperature and salinity data at the 7 and 12 m sites were collected roughly every 2 m throughout the water column using SBE-37 MicroCATs (SeaBird Electronics). Additional data were collected using Onset TempPros so that vertical resolution is $\sim$1 m for temperature.

2.1.4. Satellite-Derived Sea Surface Temperature (2005–2013)

Gridded sea surface temperature (SST) data from the Advanced Very High Resolution Radiometer (AVHRR) were obtained through the Mid-Atlantic Regional Association Coastal Ocean Observing System (http://tds.

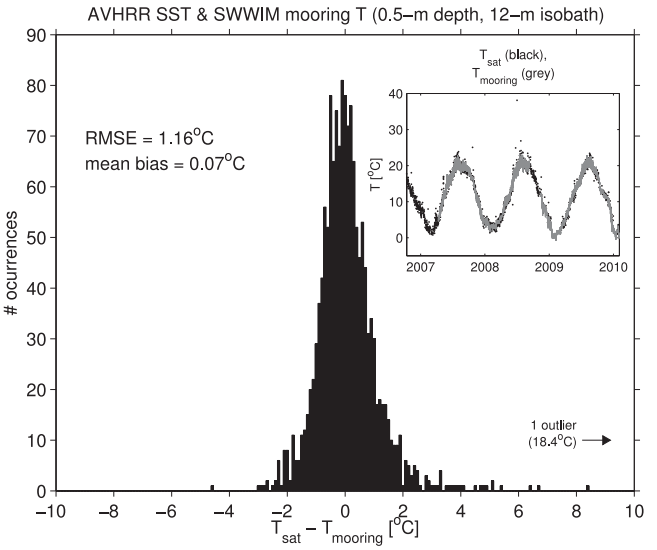

Figure 2. Comparison of SST observed by the AVHRR satellite (T_{sat}) with mooring observations at 0.5 m depth ($T_{mooring}$) on the 12 m isobath at MVCO. Histogram shows the number of occurrences of satellite error, $T_{sat} - T_{mooring}$, in 0.1°C bins. Inset in top right shows time series of T_{sat} (black dots) and $T_{mooring}$ (gray lines).

maracoos.org/thredds/SST.html, Matthew Oliver, University of Delaware). The 1 km grid resolution is similar to the AVHRR's nominal 1.1 km nadir resolution. Data are flagged as clouds based on comparisons with climatology and satellite passes in the previous 72 h. To evaluate error in the AVHRR data near land over the inner shelf, the satellite-derived SST data are compared with in situ data at the location of the MVCO node (Figure 2). During the 2006–2010 SWWIM deployment, in situ data are available near the surface at 0.5 m depth. The root-mean squared error (RMSE) is 1.16°C. The mean bias is much smaller, 0.07°C, which indicates that the AVHRR data are accurate and that error results primarily from lack of precision.

2.2. Analysis

2.2.1. Calculation of Seasonal and Annual Anomalies

For the purposes of comparing interannual temperature variability at locations across the MAB (section 3.1.), seasonal and annual anomalies are calculated using the same averaging and data availability criteria as *Shearman and Lentz* [2010]. Monthly averages are calculated only for months where at least 23 days of data are available. These monthly averages are used to calculate the seasonal cycle at each location, which is then removed to form monthly anomalies. Annual anomalies are calculated by averaging the monthly anomalies for years in which at least 9 months of data are available. Winter anomalies are calculated for years in which at least 2 months of data are available from January, February, and March. Because this study focuses on interannual variability, a linear trend is removed from each time series before computing correlation coefficients. The calculated trends are not reported in this study because the record lengths vary between sites and are influenced differently by decadal variability in some cases. The studies of *Nixon et al.* [2004] and *Shearman and Lentz* [2010] address the topic of long-term trends in the MAB.

2.2.2. Heat Balance at a Single Isobath

During 2001–2013, data from the MVCO node are used to evaluate the heat balance:

$$\frac{1}{H\Delta t}\int_{t_1}^{t_2}\left[\int_{-H}^{0}\frac{\partial T}{\partial t}\mathrm{d}z=\frac{Q}{\rho_o c_p}-\int_{-H}^{0}\frac{\partial(uT)}{\partial x}\mathrm{d}z-\int_{-H}^{0}\frac{\partial(vT)}{\partial y}\mathrm{d}z\right]\mathrm{d}t, \quad (1)$$

where T is temperature, H is the bottom depth, Δt is the total time of integration from t_1 to t_2, c_p is the heat capacity of seawater (assumed constant), Q is the surface heat flux, u is net (Eulerian + Stokes) cross-shelf velocity, and v is net along-shelf velocity. Changes in depth-averaged temperature on the left-hand side of (1) are associated with the surface heat flux and divergences of the cross-shelf and along-shelf heat fluxes. This equation is simplified as

$$\Delta T^* = T_Q^* + T_x^* + T_y^*. \quad (2)$$

An asterisk (*) is used to distinguish between the terms in this balance and the budget described below, which is integrated over an area that extends to shore.

2.2.3. Heat Budget for a Cross-Shelf Area

Data from the SWWIM cross-shelf mooring array during the more limited period 2006–2010 can be used to evaluate changes in temperature for a cross-shelf area that extends from the 12 m isobath to shore, instead

of a single isobath. Since thermal stratification data are available during these years, this approach allows the contribution of cross-shelf heat fluxes to be evaluated in a manner similar to *Fewings and Lentz* [2011], but for a greater number of years.

As described in detail by *Dever and Lentz* [1994], a heat budget is considered for a cross-shelf area, A. In the cross-shelf direction, this area is bounded by the coast at $x = 0$ and extends offshore out to an open boundary $x = L$. In the vertical direction, the area extends from the sea surface at $z = 0$ to the bottom at $z = -H$. As in *Fewings and Lentz* [2011], advection of heat is associated with the net sum of the Eulerian velocity and the Lagrangian Stokes velocity induced by surface gravity waves. The budget of area-averaged temperature, integrated from time $t = t_1$ to t_2, can be described by

$$\frac{1}{A\Delta t}\int_{t_1}^{t_2}\left[\int_0^L\int_{-H}^0 \frac{\partial T}{\partial t}\mathrm{d}z\mathrm{d}x = \frac{1}{\rho_o c_p}\int_0^L Q\mathrm{d}x - \int_{-H}^0 \tilde{u}\tilde{T}|_{x=L}\mathrm{d}z - \int_0^L\int_{-H}^0 v\frac{\partial T}{\partial y}\mathrm{d}z\mathrm{d}x - \int_0^L\int_{-H}^0 \tilde{T}\frac{\partial v}{\partial y}\mathrm{d}z\mathrm{d}x\right]\mathrm{d}t, \tag{3}$$

where $\tilde{}$ denotes removal of the spatial average. The terms in (3) are simplified as

$$\Delta T = T_Q + T_x + T_y + T_v, \tag{4}$$

where ΔT is the change in area-averaged temperature from time t_1 to t_2, and the terms on the right-hand side are the expected changes in area-averaged temperature associated with the cumulative heat flux through the ocean surface (T_Q), cross-shelf heat fluxes (T_x), advection of along-shelf velocity gradients (T_y), and along-shelf velocity divergence (T_v). The terms T_x, T_y, and T_v represent the contributions from ocean circulation.

2.2.4. Observational Estimates of Terms

The heat balance (1) is used to analyze interannual variability during the entire 2001–2013 period when data are available at the MVCO node. During this period, data are available to estimate the surface heat flux (T_Q^*) and along-shelf advection (T_y^*) terms. During the 2006–2010 SWWIM deployments, when observations are available throughout the water column at both the 7 and 12 m isobaths, the surface heat flux (T_Q), along-shelf advection (T_y) and cross-shelf heat flux (T_x) terms in the heat budget (3) are estimated for the area extending from shore to the 12 m isobath.

2.2.4.1. Surface Heat Flux

To compute the net heat flux across the ocean surface, observations of air temperature, relative humidity, air pressure, and downward short-wave and long-wave radiation are used first from ASIT where available, then the beach or shore laboratory. Because sea surface temperature is usually not available at MVCO, near-bottom temperature at the MVCO node is used to approximate sea surface temperature in the computation of surface heat fluxes. When near-bottom temperature data are unavailable at the node, a linear regression of sea surface temperature at Woods Hole is used. Since the focus of this study is the weakly stratified months, use of bottom temperature instead of SST at MVCO introduces only small biases into the surface heat flux calculation. During winter months, the surface is typically cooler than the bottom by $\sim$0.3°C due to stability provided by salinity stratification [*Fewings and Lentz*, 2011]. During the SWWIM field program, when in situ SST data are available, the error in the surface heat flux associated with using near-bottom temperature at the 12 m isobath is at most 3 W m^{-2} when averaged over the period December–February in four different winter seasons (not shown). This is equivalent to an error of $\sim$0.5°C when integrated over 3 months.

Net short-wave radiation, accounting for the albedo of the sea surface, is estimated from the empirically-derived tables of *Payne* [1972]. Net downward longwave radiation is calculated following *Dickey et al.* [1994]. Latent and sensible heat fluxes are calculated using bulk flux algorithms [*Fairall et al.*, 2003]. In calculating the heat budget, estimates of Q are assumed to be representative of the entire inner shelf from the 12 m isobath to shore.

2.2.4.2. Along-Shelf Advection

The along-shelf temperature gradient south of MVCO is estimated from AVHRR satellite SST. Grid points with bottom depths 10–14 m are used to estimate the mean seasonal sea surface temperature along the

12 m isobath in 2 month blocks from September–April. Because cloud cover is greatest during this season, robust estimates of the along-shelf SST gradient are not available for each individual year. The surface temperature gradient is assumed to extend through out the water column since this is the time of year when the water column is least stratified and the sea surface temperature best approximates the depth-averaged temperature (see section 2.2.4). In order to include only images that are useful for calculating spatial gradients, only images with $\leq$ 5% cloud cover over the analysis region are included in averages. Images from the same day are averaged together and treated as one independent sample.

The depth-averaged velocity and bimonthly seasonal means derived from the satellite SST are used to calculate $v\partial T/\partial y$ at each site, which means that the estimated interannual variability in the along-shelf advection term is primarily due to variability in the along-shelf velocity. For the heat budget during 2006–2011, periods when velocity data are not available from either the 7 or 12 m site are filled in using a regression between the two sites (R^2=0.67, not shown). Data from the 12 m site are unavailable during the periods 24 February to 1 March 2007 and 15 January to 1 March 2009. Data from the 7 m site are unavailable during the period 6 January to 5 February 2010, at which point the SWWIM field program ended. Use of the velocity regression instead of the velocity data from both sites results in differences of 0.7°C or less integrated over a 3 month period. The along-shelf advection term is only calculated during the period November–February, a period where thermal stratification is not apparent in the seasonal cycle [*Lentz*, 2008b]. Before integrating in the across-shelf direction, the depth-averaged velocity is linearly interpolated between the 7 and 12 m isobaths, and values from the 7 m site are extended inshore to the coast.

Along-shelf gradients in along-shelf velocity are assumed to be negligible so that $\partial(vT)/\partial y = v\partial T/\partial y$ in the heat balance (1), and T_v=0 in the heat budget (4). At the regional scale of the MAB, the mean along-shelf velocity varies primarily in the cross-isobath direction and along-shelf variations in along-shelf velocity are typically $<$0.05 m s^{-1} [*Lentz*, 2008a]. However, the mean along-shelf velocity varies over short scales ($\sim$10–20 km) near MVCO due to tidal rectification [*Ganju et al*., 2011; *Kirincich et al*., 2013]. Although the tidal rectification process is not expected to vary on the interannual time scales considered in this study, it is possible there may be interaction between wind-driven currents and the complex local bathymetry that would cause interannual variations in the divergence of along-shelf velocity. Since this term cannot be evaluated with the available data, it is a potential topic for future study using observations or numerical models that resolve short along-shelf scales over multiple years.

2.2.4.3. Cross-Shelf Heat Flux

Since thermal stratification data are not available for much of the period 2001–2013, the T_x^* term is not evaluated for the heat balance during this entire period. However, in order to estimate the cross-shelf heat flux during multiple years, the term T_x is evaluated for the heat budget during 2006–2011 when thermal stratification data are available. As in *Fewings and Lentz* [2011], the theoretical Stokes drift profile is estimated from the wave characteristics measured at the MVCO node in order to calculate the net (Eulerian + Stokes) cross-shelf velocity, *u*.

3. Results

3.1. Winter Temperature Anomalies in the MAB

Three shallow measurement sites on the inner shelf span the alongshore distance of the MAB during the period 1984–2013: the FRF pier, buoy 44009 and MVCO (Figure 1a). The detrended time series of winter temperature anomalies from these sites show a high degree of correlation ($R^2 > 0.8$, Figure 3), despite being separated by along-shelf distances of up to 750 km. Regression slopes *m* (not shown) and their 95% confidence intervals are estimated using a geometric mean regression [*Ricker*, 1984]. Slopes of the regressions with FRF are significantly different from one at buoy 44009 (m=1.4) and MVCO (m=1.5) where values greater than one indicate greater variability further south at FRF.

Comparison of winter temperature anomalies at FRF with all other measurement sites shows that the strongest correlations are with the shallow sites on the inner shelf (Figure 4a). Deeper sites in much closer proximity to FRF (e.g. buoys 41025 and 44014) are significantly, but more weakly, correlated. Similarly, the winter temperature anomalies at MVCO are significantly correlated with those at the closest measurement site at buoy 44008 (R^2 = 0.56, not shown), but not as strongly as with those at other inner-shelf locations. Therefore, in addition to alongshore separation, bottom depth is a major factor determining the correlation of interannual temperature anomalies at different locations in the MAB.

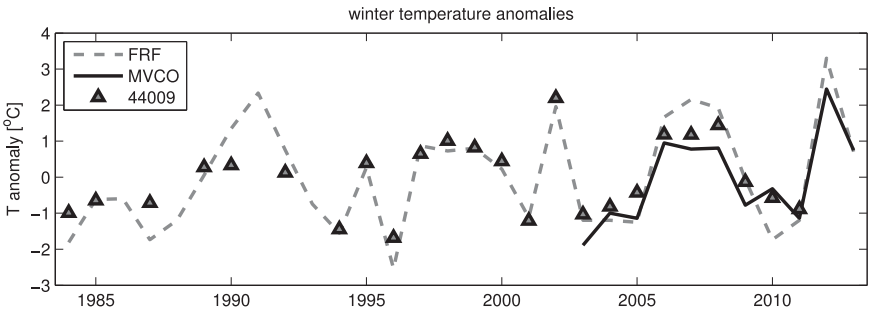

Figure 3. Time series of winter temperature anomalies from three inner-shelf locations in the MAB: FRF pier (7 m bottom depth), MVCO (12 m bottom depth), and NBDC buoy 44009 (28 m bottom depth).

Winter anomalies in the *Shearman and Lentz* [2010] SST data, using the 31 stations north of Cape Hatteras with at least 20 years of data, show a similar relationship when compared with the longest available time series at Woods Hole (Figure 4a). Although correlations are generally lower than those calculated from the more recent data in 1984–2013, the strongest correlations occur inshore of the 40 m isobath. In addition, the regression slopes at the southern end of the MAB are significantly greater than one, confirming that the magnitude of the correlated interannual variability is greater at stations further south. This pattern of enhanced variability in winter ocean temperatures at the southern end of the MAB is consistent with previous analysis of hydrographic data [*Mountain and Taylor*, 1998].

At the inner-shelf locations, winter temperature anomalies are important because they are a major factor in determining annual anomalies averaged over the entire year (Figure 5a). At FRF and MVCO, the detrended winter temperature anomalies account for 69–77% of the variance in the annual temperature anomalies. The winter anomalies are larger in magnitude than the annual anomalies, as indicated by regression slopes of 0.41–0.56. The annual anomalies are correlated with, and smaller than the winter anomalies because the variability between years is strongest during the winter season. The wintertime anomalies cannot persist into summer because the flushing time of the inner shelf is on the order of days [*Fewings et al.*, 2008].

The detrended winter ocean temperature anomalies at FRF and MVCO are also correlated with local air temperature anomalies at both locations (Figure 5b). The winter air temperature anomalies account for 53–62% of the variance in the winter ocean temperature anomalies. The regression slopes of 0.83–0.96 are not

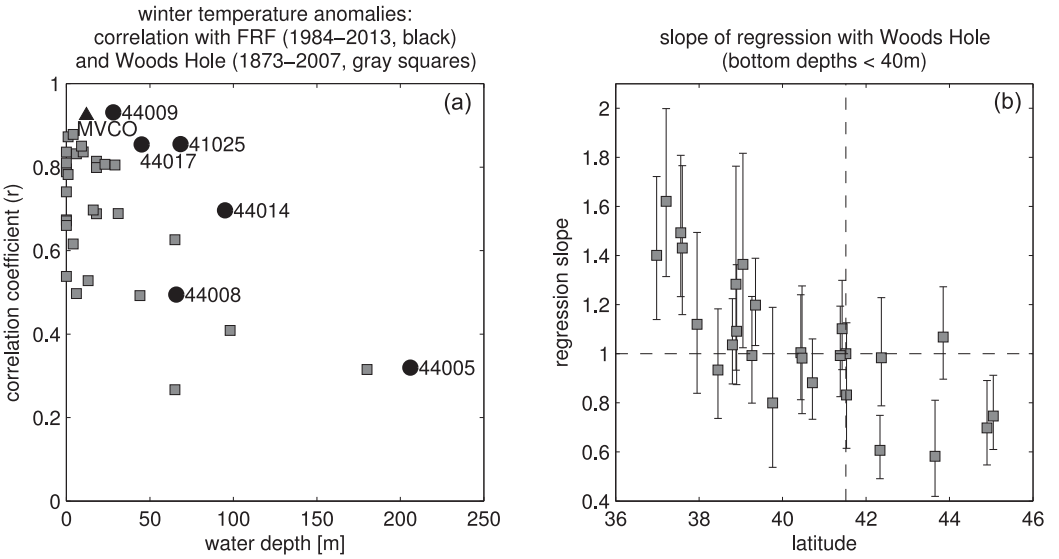

Figure 4. (a) Correlation of winter temperature anomalies at stations of different bottom depth with those at the FRF pier in Duck, NC during 1984–2013 (black) and Woods Hole during 1873–2007 (gray squares). Circles indicate sea surface temperature from NDBC buoys and triangle represents near-bottom data from the MVCO node. (b) Slope of the regressions with Woods Hole at locations of different latitude, inshore of the 40 m isobath. Error bars indicate 95% confidence intervals. Vertical dashed line indicates the latitude of Woods Hole and horizontal dashed line indicates a regression slope of one. Values greater than one indicate weaker variability at Woods Hole.

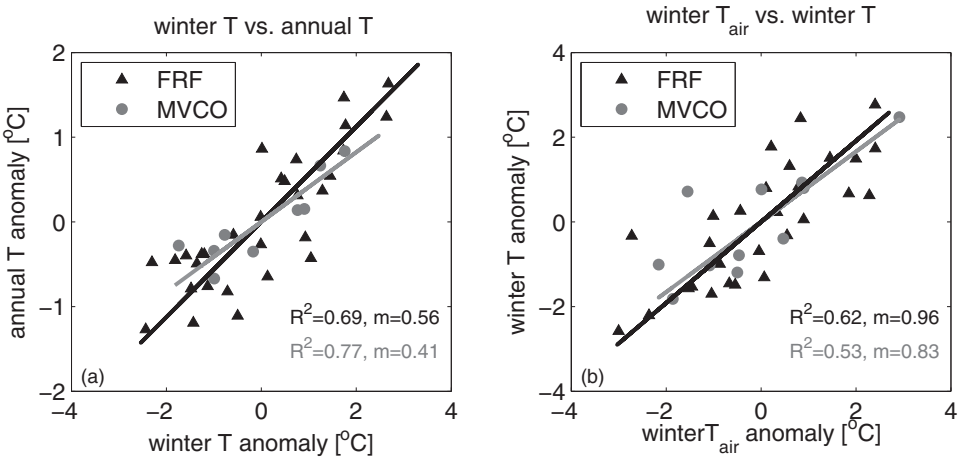

Figure 5. Correlation between winter ocean temperature anomalies with (a) annual ocean temperature anomalies and (b) winter air temperature anomalies. Black triangles indicate SST at the FRF site, and gray circles indicate near-bottom temperature at the MVCO site. Correlations (R^2) and regression slopes (m) are shown in the lower right corner for both FRF (black) and MVCO (gray). All correlations shown are significant at the 95% confidence level. Note the difference in scale of the *y* axes between the two plots.

significantly different from one at either site. The significant correlation between oceanic and air temperatures at both locations suggests that the broad alongshore scales of variability in oceanic temperature are associated with broad scales of atmospheric variability.

3.2. Heat Balance at the New England Inner Shelf: 2001–2013

Using data from the 12 m isobath at MVCO, terms of the heat balance (2) are analyzed to assess whether changes in temperature over the course of the unstratified winter season are completely balanced by the surface heat flux. It is shown that (1) there is a residual warming that is not balanced by the surface heat flux over the course of the seasonal cycle, and (2) that along-shelf advection can account for the interannual variability of this residual heat flux.

The heat balance terms are estimated for 2 month periods during which temperature, surface heat flux, and along-shelf velocity data are concurrently available over at least 50% of the total record length. This threshold for data availability was chosen to be high enough that averages are not dominated by single events at weather-band periods (~5 d). The 2 month averaging period is chosen to ensure that the estimates do not include physical processes from multiple seasons. All averages are expressed as the cumulative change in temperature over a 2 month period (°C/60 d).

3.2.1. Seasonal Cycle

Late fall and winter months at MVCO are characterized by relatively strong eastward wind stress τ^y compared with summer months, and a small offshore component τ^x (Figure 6a). The depth-averaged along-shelf velocity has a westward mean that opposes the mean eastward wind stress (Figure 6b). Decreased westward flow during winter is consistent with a significant influence of along-shelf wind stress on the seasonal cycle of alongshore velocity at this location [*Lentz*, 2008b]. Standard deviations of the bimonthly means, which indicate the amount of variance at interannual time scales, are greatest during winter for both wind and along-shelf velocity (Figures 6a and 6b).

The bimonthly estimates of cumulative surface heat flux (T_Q^*) indicate that the loss of heat due to air-sea fluxes during October–February is not as great as the heat gain during April–September (Figure 6c). Observed changes in water temperature (ΔT^*) do not follow the seasonal cycle of the cumulative surface heat flux. The residual of these terms shows cooling due to oceanic advection during May–October, and a smaller warming during November–March (Figure 6d). The summertime cooling can be explained by cross-shelf heat fluxes associated with an upwelling circulation [*Fewings and Lentz*, 2011]. It will be shown in the following sections that the wintertime warming is associated with along-shelf advection rather than cross-shelf heat fluxes.

3.2.2. Interannual Variability

If interannual variability in temperature were completely driven by local atmospheric conditions, the cumulative temperature change (ΔT^*) would be completely accounted for by the cumulative surface heat flux

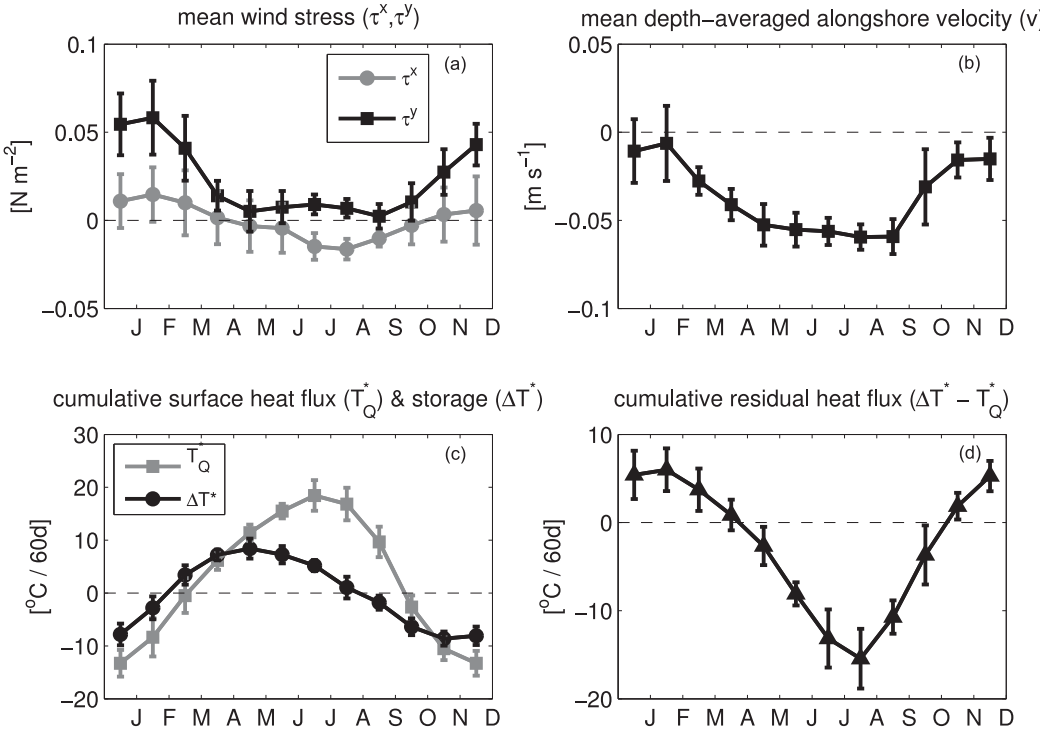

Figure 6. Seasonal cycles at MVCO. (a) Bimonthly means of cross-shelf (τ^x, gray) and along-shelf (τ^y, black) components of the wind stress. Error bars represent the standard deviation of means from different years. Note that the bimonthly means are shown at monthly intervals, and the first point on the left of each plot represents a December–January mean. (b) Bimonthly means of depth-averaged along-shelf velocity (v). (c) Cumulative surface heat flux (T_Q^*, gray) and storage (ΔT^*) over 2 month intervals. (d) Cumulative residual heat flux over 2 month intervals ($\Delta T^* - T_Q^*$), which theoretically must be balanced by oceanic advection.

(T_Q^*). Observed averages of these two terms from different years are significantly correlated during both the November–December and January–February periods (Figure 7a). The regression slopes of less than one indicate that T_Q^* predicts greater cooling than observed. The regression slope decreases from 0.85 during November–December to 0.46 during January–February. To ensure that results are not affected by sampling different parts of the seasonal cycle during different years, it has been checked that averages of ΔT^* and T_Q^* are not significantly correlated with the average year day of the available data. The deviations from a one-dimensional balance between ΔT^* and T_Q^* suggest that oceanic advection warms the inner shelf at this location, particularly during years with strong surface cooling, and therefore has a significant influence on the heat balance at seasonal and interannual time scales.

The importance of along-shelf advection is assessed by examining whether estimates of T_y^* account for the deviations from a one-dimensional balance between ΔT^* and T_Q^*. Bimonthly seasonal averages of satellite SST data show that there is a strong ($\sim -0.04^\circ$C km^{-1}) along-shelf temperature gradient to the west of the MVCO node during November–February (Figure 8). The along-shelf SST gradients are weak during the periods September–October and March–April, but these periods are also more likely to be influenced by thermal stratification during fall and early spring. The mean along-shelf gradient to the west of the node during November–February is associated with a localized front that is oriented from northwest to southeast and crosses isobaths, intersecting the coastline (Figure 9a). SST snapshots show spatial variability in this front, which may be associated with instabilities (Figure 9b). Weak gradients to the east of the MVCO node are associated with a SST minimum between the two islands of Martha's Vineyard and Nantucket. To account for the asymmetrical wintertime temperature gradient near the MVCO node, the strong gradient to the west of the node is used to calculate T_y^* when the velocity is eastward and the weaker gradient to the east of the node is used when the velocity is westward.

The estimated along-shelf advection at MVCO is positive during each period analyzed during November–February (Figure 7b), accounting for much of the cold bias that occurs when only surface heat flux is included and advection is neglected. Warming due to along-shelf advection is therefore an important part of the mean wintertime heat balance. During November–December, the estimated along-shelf advection

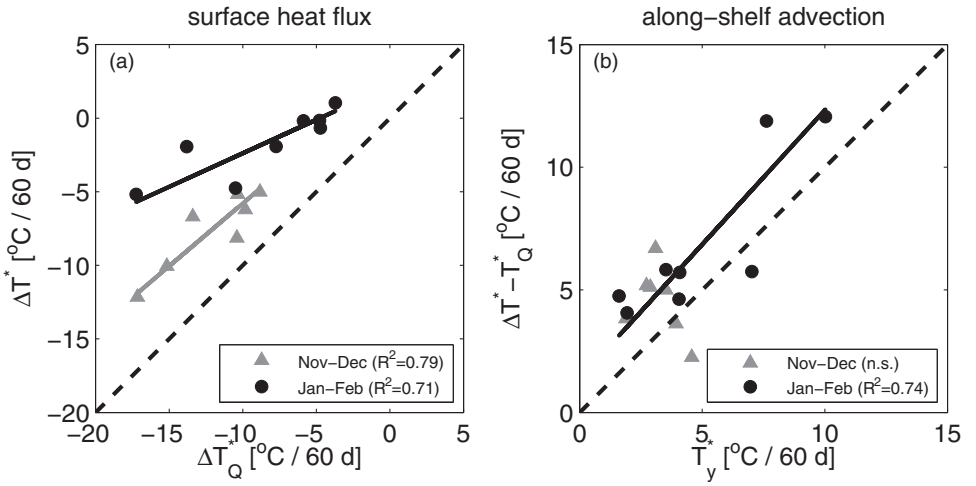

Figure 7. Comparison of estimated heat balance terms integrated over the periods November–December (gray triangles) and January–February (black circles) during different years at MVCO. (a) Cumulative surface heat flux (T_Q^*) compared with cumulative change in temperature (ΔT^*). (b) Cumulative along-shelf advection (T_y^*) compared with the difference between cumulative temperature change and time-integrated surface heat flux ($\Delta T^* - T_Q^*$). Black-dashed lines represent equality. Regression lines and R^2 values are shown where correlations are significant at the 95% confidence interval, and "n.s." indicates that the correlation is not significant.

does not account for the variability in the deviations from a one-dimensional balance. As discussed further in section 3.3., it is possible that cross-shelf advection can account for part of the residual variance. In addition, the estimated along-shelf advection only accounts for interannual variations in along-shelf velocity acting on the seasonal mean along-shelf temperature gradient. Interannual variability in the along-shelf temperature gradient or the divergence of along-shelf velocity may also explain the portion of the residual variance. However, the residual variance that cannot be accounted for during November–December is relatively small compared with the variance of the cumulative temperature change and that of the cumulative surface heat flux.

During January–February, the correlation between T_y^* and $\Delta T^* - T_Q^*$ is significant. The relative importance of surface heat flux and along-shelf advection is not sensitive to the specific 60 day integration time scale chosen for the analysis. Using a longer period January–March instead of January–February results in slightly stronger correlation coefficients and similar regression slopes (within 10%) compared with those shown in Figure 6. January–February is the time of year when eastward (positive) along-shelf velocity is most likely to occur at this location (Figure 6b). Therefore, the seasonally induced gradients to the west (Figure 8) are more likely to affect the Martha's Vineyard inner shelf during these months.

The relationships between cooling, surface heat flux, and along-shelf advection during January–February suggest a common link to the along-shelf wind stress, since the along-shelf components of wind stress and depth-averaged velocity are correlated in the MAB [*Lentz*, 2008b]. The cumulative along-shelf wind stress at MVCO is positively correlated with the estimated along-shelf advection T_y^*, and inversely correlated with both the cumulative surface heat flux T_Q^* and the storage term ΔT^* ($R^2 = 0.83$–0.85, not shown). In addition, the surface heat flux is strongly correlated with the air-sea temperature difference (Figure 10). Specifically, the latent and sensible components of the surface heat flux are significantly correlated with the air-sea temperature difference, and seasonal differences in short-wave radiation and latent heat flux account for most of the offset between the two periods (not shown). As discussed further in section 4, the relationship between the surface heat flux and air-sea temperature difference has implications for the time scales of ocean temperature variability at different water depths over the shelf.

3.3. Heat Budget Inshore of the 12 m Isobath: 2006–2011

The previous section showed that warming associated with along-shelf advection can account for the residual between cumulative surface heat flux and changes in water temperature during winter at MVCO. However, because thermal stratification data are not available at MVCO during much of the period analyzed, the heat balance analysis during the period 2001–2013 cannot rule out cross-shelf heat flux as a factor in determining wintertime temperatures. *Fewings and Lentz* [2011] show that there can be a small amount of

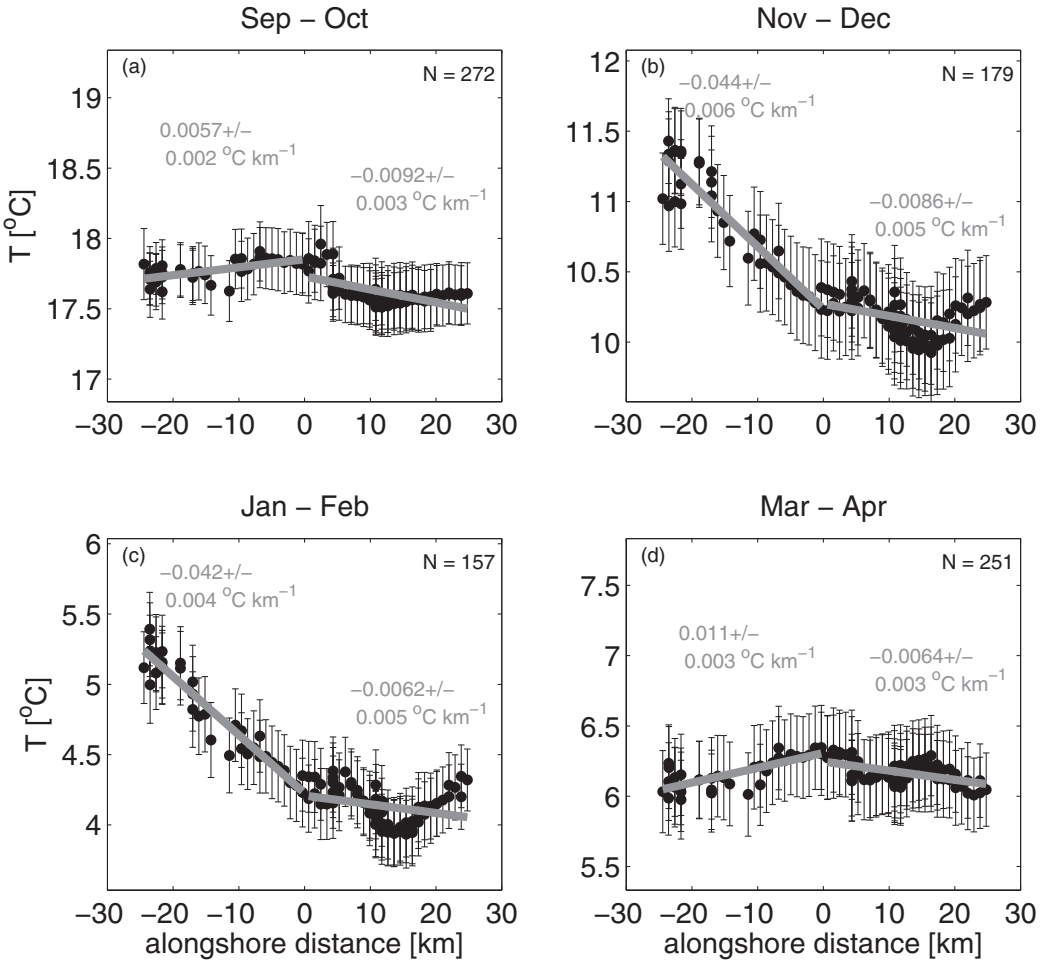

Figure 8. Seasonal mean AVHRR SST (2005–2013) between the 10 and 14 m isobaths south of Martha's Vineyard during (a) September–October, (b) November–December, (c) January–February, and (d) March–April. Number of independent observations, N, are indicated in the top right corners. Error bars indicate 95% confidence intervals. Alongshore distance $y = 0$ corresponds to the MVCO node. Separate linear regressions east and west of the MVCO node are shown in gray, with estimated alongshore temperature gradients.

warming due to cross-shelf heat fluxes associated with upwelling during winter months, when the surface is slightly colder than the bottom.

To test whether cross-shelf heat fluxes can provide an alternative explanation for the residual between surface heat flux and temperature change, the heat budget (4) is analyzed during four different winters. Terms are integrated starting 3 December when data are available during all 4 years. Along-shelf advection

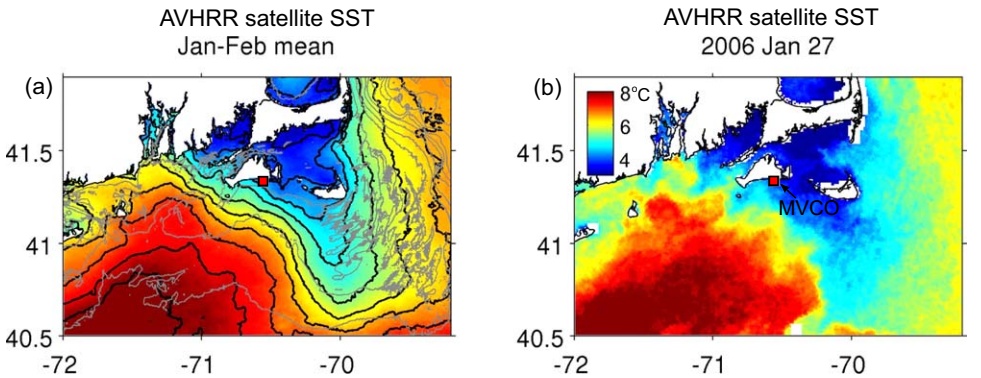

Figure 9. (a) Seasonal mean AVHRR SST (2005–2013) during January–February. Black contours indicate 0.5°C intervals. (b) Snapshot of AVHRR SST on 27 January 2006. Red square indicates location of MVCO.

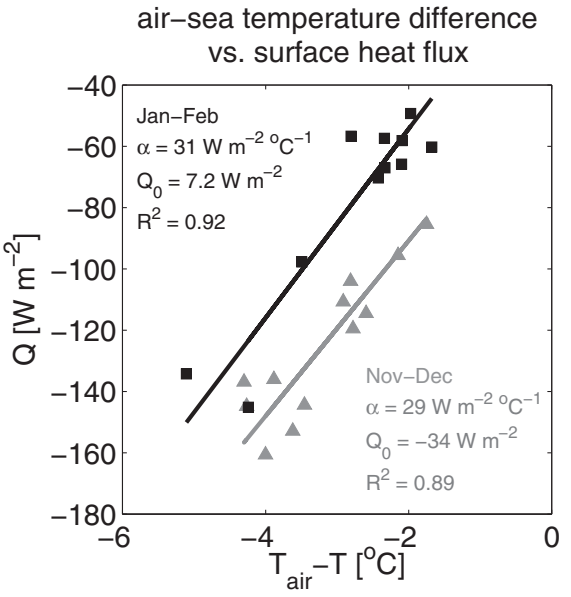

Figure 10. Regression between the mean air-sea temperature difference ($T_{air} - T$) and calculated surface heat flux (Q) for periods November–December (gray, triangles) and January–February (black, squares). Regression slopes (α), intercepts (Q_o), and correlations (R^2) are shown for each period.

accounts for the residual term, $\Delta T^* - T_Q^*$, within ~2°C (Figure 11). Cross-shelf heat fluxes are relatively small during all years analyzed, providing further evidence that wintertime temperature variability at this location is determined primarily by surface heat flux and along-shelf advection.

Cross-shelf heat fluxes have the greatest influence during January 2010, which is characterized by a strong upwelling circulation, thermal stratification, and offshore wind stress compared with other years analyzed (Figure 12). The cumulative surface heat flux is smaller in January 2010 than the other years (not shown), so the increased vertical temperature gradient is likely

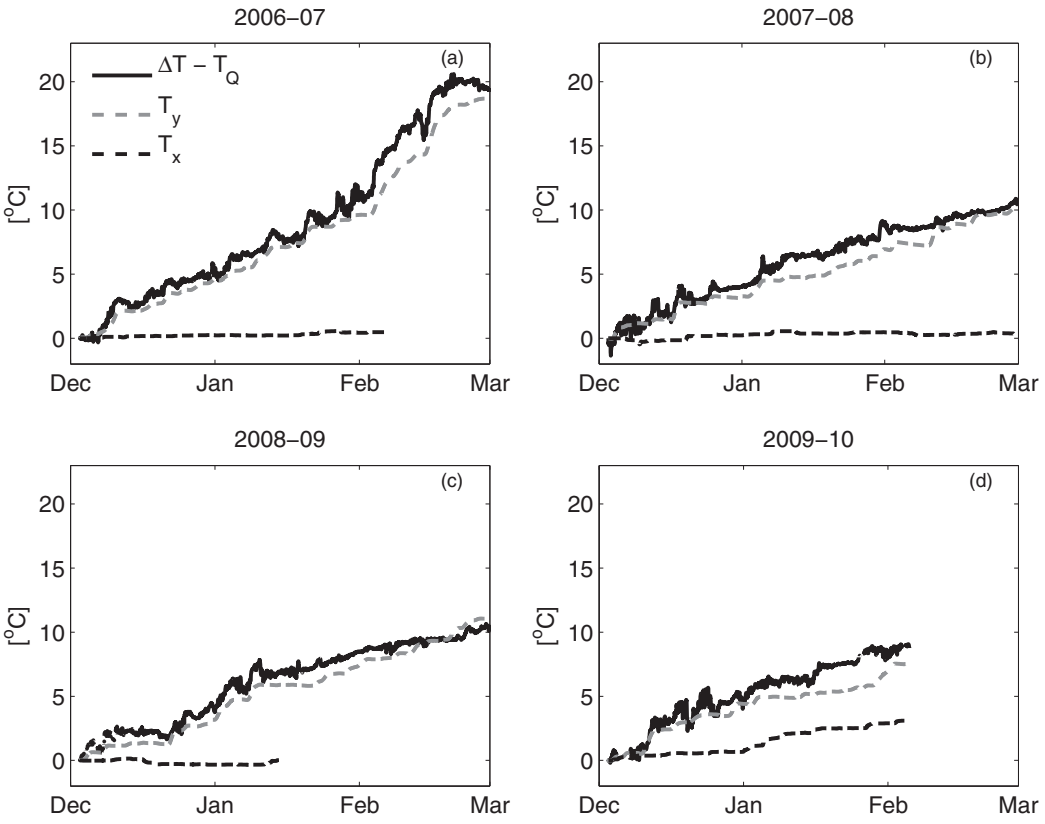

Figure 11. Calculated heat budget terms from 3 December to 1 March during fall–winter periods when thermal stratification data are available: (a) 2006–2007, (b) 2007–2008, (c) 2008–2009, and (d) 2009–2010. The cumulative residual of storage and surface heat flux ($\Delta T - T_Q$, black) along-shelf advection (T_y, gray-dashed) and cross-shelf heat flux (T_x, black-dashed) are calculated beginning on 3 December.

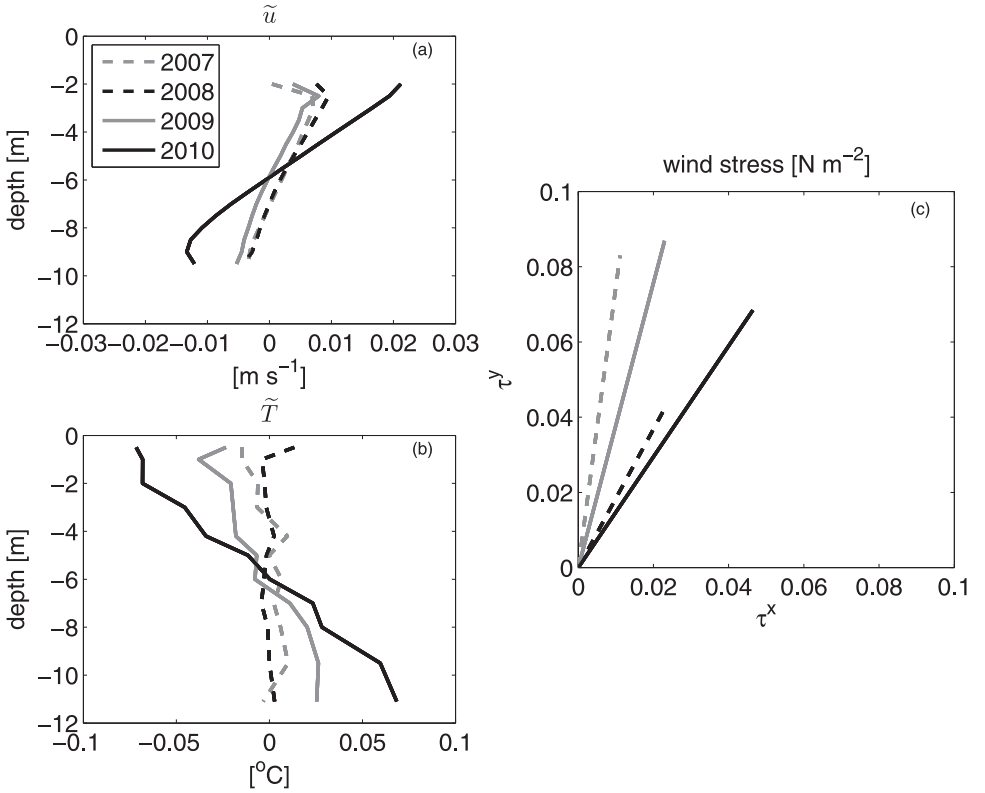

Figure 12. January averages of (a) depth-dependent cross-shelf velocity ($\tilde{u}$), (b) depth-dependent temperature ($\tilde{T}$), and (c) wind stress during years when thermal stratification data are available. The depth-dependent profiles (Figures 12a and12 b) have depth-averaged values removed. Wind stress components (Figure 12c) are shown as vectors.

associated with advection of cold water over warm water by the upwelling circulation. The presence of cold water over warm water can be maintained in shallow waters of the MAB, where salinity gradients provide stability [*Fewings and Lentz*, 2011]. Stronger offshore winds may therefore produce a greater warming of the water column during winter. The resulting warming is always likely to be small at this location compared with surface heat flux and along-shelf advection, but may be large enough to account for the residuals of ~2°C that occur over 2 month periods (Figure 7b). It is also possible that these unexplained residuals can be explained by processes that are neglected in the present estimate of along-shelf advection, such as interannual variability of the along-shelf temperature gradient and/or temperature variability associated with the divergence of along-shelf velocity.

4. Discussion

This study extends previous work on temperature variability over the inner shelf to interannual time scales. It is shown that winter temperature anomalies have broad along-shelf scales, and explain much of the variability in the annual temperature anomalies in the MAB (Section 3.1). This means that the processes associated with winter cooling are particularly important for interpreting climate variability in ocean temperature records from nearshore locations. Wintertime air temperatures have broad scales of correlation throughout the eastern U.S., but the predictive power of climate indices such as the North Atlantic Oscillation varies over long multidecadal time scales [*Joyce*, 2002]. *Chen et al*. [2014] show that winter ocean temperature anomalies over the New England shelf are correlated with the latitude of the jet stream, which plays an important role in determining wind strength and direction, as well as the air temperature. Long-term shifts in the position and variability or the jet stream may therefore alter the magnitude and spatial patterns of interannual temperature variability in the MAB.

The availability of data on interannual time scales provides new insight into the potential importance of along-shelf advection at seasonal time scales on the inner shelf. From one season (2004–2005) on the Martha's Vineyard inner shelf, *Fewings and Lentz* [2011] inferred a one-dimensional balance between the

cumulative change in temperature and surface heat flux during winter. In the context of interannual variability, that particular winter is found to have a relatively small influence of alongshore advection. Advective warming of only 4.7°C over 60 days is estimated during January–February 2005, compared with an average of 6.8°C over all years and a maximum of 12.1°C during 2007. At seasonal time scales, along-shelf advection has also been shown to be an important process over the North Carolina inner shelf at FRF during the winter [*Austin*, 1999]. However, along-shelf advection cools the inner shelf during winter at FRF because cold fronts are typically associated with a southward component of wind stress, leading to along-shelf advection of colder water from the north.

In addition to influencing seasonal variability, it is shown in sections 3.2 and 3.3 that along-shelf advection varies significantly between different winters at MVCO. Along-shelf velocity on the inner shelf is tightly coupled with the along-shelf component of wind stress. If strong along-shelf temperature gradients are present, interannual variability in the magnitude of along-shelf wind stress leads to differences between years in the importance of along-shelf advection. At MVCO in the northern MAB, there is an inverse correlation between along-shelf advection and cumulative surface heat flux during different winters. Anomalous eastward wind stress is associated with stronger surface cooling, but also drives advection of warmer water from the west. In the southern MAB, the coastline is orientated in the north-south direction instead of east-west. At these locations, atmospheric cold fronts that cause surface cooling are associated with southward wind stress [*Austin and Lentz*, 1999]. This southward wind stress advects cooler water from the north so that along-shelf advection is positively correlated with surface heat flux in the southern MAB [*Austin*, 1999]. Along-shelf advection can therefore have opposite relationships with the wintertime surface heat flux in different parts of the MAB.

The along-shelf temperature gradient observed during winter to the west of MVCO ($\sim 4 \times 10^{-5}$°C m^{-1}) is an order of magnitude larger than estimates of the mean along-shelf gradient throughout the entire MAB. *Lentz* [2010] estimates that the mean along-shelf temperature gradient has magnitude 2×10^{-6}°C m^{-1} at the 70 m isobath and 4×10^{-6}°C m^{-1} further inshore at the 30 m isobath. From historical SST data, at locations that are primarily close to shore, *Shearman and Lentz* [2010] estimate a mean gradient of magnitude 6.4×10^{-6}°C m^{-1}, which is larger in summer and smaller during winter. The mean and seasonal variability of this along-shelf SST gradient correspond closely with the along-shelf gradient of air temperature throughout the MAB [*Shearman and Lentz*, 2010]. *Austin* [1999] estimates that the along-shelf temperature gradient on the North Carolina inner shelf has a larger magnitude, 1.2×10^{-5}°C m^{-1}. If local along-shelf gradients are weak, on the order of the mean gradient along the entire MAB, the temperature change due to along-shelf advection would only be $\sim$1°C over a 2 month period. In this case, the shallow water of the inner shelf favors surface heat flux as the dominant process balancing temperature variability during the unstratified season. However, if strong along-shelf gradients occur at local scales, along-shelf advection may make an important contribution to the heat budget over the inner shelf. In addition to the study site at MVCO, along-shelf advection likely contributes to the wintertime heat budget at other locations where coastline and bathymetry vary on relatively short ($<$100 km) along-shelf scales.

The strong along-shelf temperature gradient at MVCO is associated with a localized temperature front to the west of MVCO. Previous analysis of satellite imagery has shown that it is more common for wintertime temperature fronts to cross isobaths on the southern New England shelf than other locations in the MAB [*Ullman and Cornillon*, 2001]. Because the local along-shelf temperature gradient is strong compared to the mean along-shelf gradient in the MAB, it is likely that the gradient is maintained by cross isobath exchange at locations to the west of MVCO, i.e. net transport of cold water offshore and warm water onshore. In addition to gradients of temperature, tidal amplitudes increase significantly from west to east across the southern New England shelf, which creates an along-shelf gradient in the strength of vertical mixing [*He and Wilkin*, 2006; *Wilkin*, 2006]. It is possible that weaker vertical mixing to the west of MVCO is associated with stronger salinity stratification, allowing wintertime upwelling to warm the water column there. However, the advection of cooler water over warm water weakens stratification and increases vertical mixing [*Horwitz and Lentz*, 2014], limiting the potential for heat gain by this process. Another possibility is that the temperature front itself is unstable, creating an onshore eddy flux of heat. The dominant terms of the heat budget vary across spatial scales of $\sim$10 km or less in this region [*Wilkin*, 2006; *Kirincich et al*., 2013]. Fully understanding the heat budget likely requires the use of three-dimensional numerical models, or velocity and temperature observations that resolve fine spatial scales, even during periods of weak stratification.

Although specific mechanisms for the development of cross-isobath fronts may be complex, the relatively short along-shelf scales over the inner shelf can be anticipated from a simplified heat balance. Results in section 3.2 show that anomalies of surface heat flux are linearly related to air and ocean temperature anomalies by $Q=Q_o+\alpha(T_{air}-T)$. With this linearized form of the surface heat flux, *Shearman and Lentz* [2010] show that oceanic temperature trends adjust to air temperature trends over an adjustment time scale $t_{adj}=\rho_o c_p H\alpha^{-1}$ when no along-shelf variations are present. Over the Martha's Vineyard inner shelf, the parameters $\alpha = 30$ W m^{-2}°C^{-1} (Section 3.2.2, Figure 10) and water depth $H = 12$ m correspond to $t_{adj} \approx 20$ days, which is longer than a storm event but shorter than the winter season. If along-shelf variations are present, then the adjustment occurs over along-shelf length scale $L=vt_{adj}$. For $v \approx 0.05$m s^{-1}, then $L \approx 80$km, which roughly corresponds to the along-shelf scale of the front observed in satellite SST to the west of MVCO. The rapid adjustment of temperature in the shallow water of the inner shelf allows for the development of along-shelf temperature gradients at much smaller along-shelf scales than locations further offshore.

Even though along-shelf advection over these relatively small (<100 km) scales has been shown to be an important part of the heat budget at MVCO, winter temperature anomalies are still correlated at locations as far away as FRF and MVCO. There are two possible reasons for the strong correlation over large along-shelf scales. One possible explanation is that both along-shelf advection and surface heat flux are correlated at opposite ends of the MAB. As discussed above, differences in coastline orientation at opposite ends of the MAB lead to different relationships between surface cooling and along-shelf advection. An inverse correlation between along-shelf advection at opposite ends of the MAB would be consistent with regressions of inner-shelf temperature shown in section 3.1, which indicate greater variability of inner-shelf temperature at interannual time scales in the southern end of the MAB. This explanation requires that the broad scale atmospheric patterns associated with surface cooling throughout the MAB also produce a strong correlation between eastward wind stress off New England, which warms the inner shelf there through along-shelf advection, and southward wind stress off North Carolina.

A more likely explanation for the large-scale correlation of nearshore temperatures in the MAB is that ocean and air temperatures are tightly coupled over the inner shelf, even in the presence of along-shelf advection. Warming of the water column due to along-shelf advection at MVCO enhances cooling of the water column by the surface heat flux. At time scales longer than t_{adj}, which is relatively short over the inner shelf, an increase in the air-sea temperature difference due to oceanic advection leads to a greater loss of heat from the ocean as it adjusts to follow the air temperature. If inner-shelf ocean temperature anomalies adjust to broad-scale air temperature anomalies regardless of the presence of along-shelf advection, the enhanced variability at the southern end of the MAB must be associated with greater variability in air temperature to the south. Consistent with this explanation, *Shearman and Lentz* [2010] show that the variability of monthly air temperature anomalies increases toward the south in the MAB. There is further evidence of greater variability in air temperature to the south in the analysis of *Deser and Blackmon* [1993]. The dominant mode of interannual variability in wintertime surface air temperature over the North Atlantic is associated with a dipole pattern, in which one center of strong variability occurs off the southern U.S. east coast.

The interannual variability of temperature at nearshore locations influences coastal marine ecosystems at local and regional scales. For example, warmer temperatures are associated with reduced magnitude of the winter-spring bloom and elevated zooplankton abundance at several semi-enclosed bays in New England [*Keller et al*., 1999, 2001]. The broad along-shelf scales of interannual temperature variability suggest that related patterns of ecosystem variability may also be coherent throughout the MAB, particularly at inner-shelf locations and in well-mixed estuaries. However, it is also possible that interannual temperature variability is associated with physical transport of nutrients and plankton communities along the coast, since interannual variability in wintertime cooling at the ocean surface is also associated with variability in wind-driven along-shelf advection over the inner shelf. This is particularly likely at locations where wintertime temperature fronts cross isobaths, like the southern New England inner shelf.

5. Conclusions

The observed interannual variability in nearshore ocean temperatures is linked to large-scale atmospheric variability in the MAB. Wintertime ocean temperatures over the inner shelf tend to adjust toward local air

temperature over a time scale of ~20 days, which is relatively short compared to the seasonal time scale. As a result, the correlation between air temperatures over broad atmospheric scales of 100s of km leads to a correlation between wintertime inner-shelf ocean temperatures throughout the MAB at interannual time scales. Wintertime processes are particularly important for interpreting regional interannual variability at nearshore locations since wintertime temperatures vary strongly between years and account for much of the variance in the annual temperature anomalies.

The results of this study indicate that the winter season is not necessarily characterized by a one-dimensional balance between the cumulative air-sea heat flux and changes in ocean temperature, despite the lack of strong stratification. Alongshore advection may contribute to the heat budget over the inner shelf and modify the surface heat flux. Whether along-shelf advection dampens or enhances surface cooling at seasonal and interannual time scales depends on the along-shelf component of wind stress associated with the dominant patterns of atmospheric variability, which varies throughout the MAB depending on whether the coastline is oriented zonally or meridionally. The magnitude of along-shelf advection likely depends on the presence of localized along-shelf variations in bathymetry and coastline, which allow temperature fronts to cross isobaths and set up localized along-shelf gradients. Observations and numerical models that resolve small horizontal scales of 10 km or less would help determine the specific processes that set up along-shelf temperature gradients on the inner shelf during winter.

Acknowledgments

Data used in this manuscript are available online at the locations specified in section 2 (Martha's Vineyard Coastal Observatory, US Army Corps of Engineers Field Research Facility, National Data Buoy Center, Mid-Atlantic Regional Association Coastal Ocean Observing System). SWWIM mooring data are available from the authors upon request. The authors thank Kipp Shearman (OSU) for compiling and providing the long-term SST data, and Anthony Kirincich (WHOI) for assistance with the satellite data. The authors also thank Matthew Oliver (U. Delaware) and MARACOOS for making the gridded AVHRR data publicly available, as well as Craig Marquette and Janet Fredericks (WHOI) for their efforts in collecting the SWWIM field data and maintaining the time series of measurements at MVCO. FRF data are provided by the Field Research Facility, Field Data Collections and Analysis Branch, US Army Corps of Engineers, Duck, North Carolina. Three anonymous reviewers helped improve the content and clarity of the manuscript. T. Connolly was supported by the Postdoctoral Scholar Program at the Woods Hole Oceanographic Institution, with funding provided by the United States Geological Survey. S. Lentz was funded by Ocean Sciences Division of the National Science Foundation, grants OCE-0548961 (SWWIM) and OCE-1332646 (ISLE).

References

Austin, J. A. (1999), The role of the alongshore wind stress in the heat budget of the North Carolina inner shelf, *J. Geophys. Res.*, *104*(C8), 18,187–18,203.

Austin, J. A., and S. J. Lentz (1999), The relationship between synoptic weather systems and meteorological forcing on the North Carolina inner shelf, *J. Geophys. Res.*, *104*(C8), 18,159–18,185.

Chen, K., G. G. Gawarkiewicz, S. J. Lentz, and J. M. Bane (2014), Diagnosing the warming of the Northeastern U.S. Coastal Ocean in 2012: A linkage between the atmospheric jet stream variability and ocean response, *J. Geophys. Res. Oceans*, *119*, 218–227, doi:10.1002/2013JC009393.

Cook, T., M. Folli, J. Klinck, S. Ford, and J. Miller (1998), The relationship between increasing sea-surface temperature and the northward spread of *Perkinsus marinus* (Dermo) disease epizootics in oysters, *Estuarine Coastal Shelf Sci.*, *46*, 587–597.

Deser, C., and M. L. Blackmon (1993), Surface climate variations over the North Atlantic ocean during winter: 1900–1989, *J. Clim.*, *6*, 1743–1753.

Dever, E. P., and S. J. Lentz (1994), Heat and salt balances over the northern California shelf in winter and spring, *J. Geophys. Res.*, *99*(C8), 16,001–16,017.

Dickey, T. D., D. V. Manov, R. A. Weller, and D. A. Siegel (1994), Determination of longwave heat flux at the air-sea interface using measurements from buoy platforms, *J. Atmos. Oceanic Technol.*, *11*, 1057–1078.

Fairall, C. W., E. F. Bradley, J. E. Hare, A. A. Grachev, and J. B. Edson (2003), Bulk parameterization of air-sea fluxes: Updates and verification for the COARE algorithm, *J. Clim.*, *16*, 571–591.

Fewings, M., S. J. Lentz, and J. Fredericks (2008), Observations of cross-shelf flow driven by cross-shelf winds on the inner continental shelf, *J. Phys. Oceanogr.*, *38*, 2358–2378.

Fewings, M. R., and S. J. Lentz (2011), Summertime cooling of the shallow continental shelf, *J. Geophys. Res.*, *116*, C07015, doi:10.1029/2010JC006744.

Ganju, N. K., S. J. Lentz, A. R. Kirincich, and J. T. Farrar (2011), Complex mean circulation over the inner shelf south of Martha's Vineyard revealed by observations and a high-resolution model, *J. Geophys. Res.*, *116*, C10036, doi:10.1029/2011JC007035.

He, R., and J. L. Wilkin (2006), Barotropic tides in the southeast New England shelf: A view from a hybrid data assimilative modeling approach, *J. Geophys. Res.*, *111*, C08002, doi:10.1029/2005JC003254.

Horwitz, R., and S. J. Lentz (2014), Inner-shelf response to cross-shelf wind stress: The importance of the cross-shelf density gradient in an idealized numerical model and field observations, *J. Phys. Oceanogr.*, *44*, 86–103, doi:10.1175/JPO-D-13-075.1.

Joyce, T. M. (2002), One hundred plus years of wintertime climate variability in the eastern United States, *J. Clim.*, *15*, 1076–1086.

Keller, A. A., C. A. Oviatt, H. A. Walker, and J. D. Hawk (1999), Predicted impacts of elevated temperature on the magnitude of the winter-spring phytoplankton bloom in temperate coastal waters: A mesocosm study, *Limnol. Oceanogr.*, *44*, 344–356.

Keller, A. A., C. Taylor, C. Oviatt, T. Dorrington, G. Holcombe, and L. Reed (2001), Phytoplankton production patterns in Massachusetts Bay and the absence of the 1998 winter-spring bloom, *Mar. Biol.*, *138*, 1051–1062.

Kirincich, A. R., S. J. Lentz, J. T. Farrar, and N. K. Ganju (2013), The spatial structure of tidal and mean circulation over the inner shelf south of Martha's Vineyard, Massachusetts, *J. Phys. Oceanogr.*, *43*(9), 1940–1958, doi:10.1175/JPO-D-13-020.1.

Lee, Y. J., and K. Lwiza (2005), Interannual variability of temperature and salinity in shallow water: Long Island Sound, New York, *J. Geophys. Res.*, *110*, C09022, doi:10.1029/2004JC002507.

Lentz, S. J. (2008a), Observations and a model of the mean circulation over the Middle Atlantic Bight continental shelf, *J. Phys. Oceanogr.*, *38*, 1203–1221, doi:10.1175/2007JPO3768.1.

Lentz, S. J. (2008b), Seasonal variations in the circulation over the Middle Atlantic Bight continental shelf, *J. Phys. Oceanogr.*, *38*, 1486–1500.

Lentz, S. J. (2010), The mean along-isobath heat and salt balances over the Middle Atlantic Bight continental shelf, *J. Phys. Oceanogr.*, *40*, 934–948.

Mountain, D. G. (2003), Variability in the properties of shelf water in the Middle Atlantic Bight, 1977–1999, *J. Geophys. Res.*, *108*(C1), 3014, doi:10.1029/2001JC001044.

Mountain, D. G., and M. H. Taylor (1998), Spatial coherence of interannual variability in water properties on the U.S. northeast shelf, *J. Geophys. Res.*, *103*(C2), 3083–3092.

Murawski, S. A. (1993), Climate change and marine fish distributions: Forecasting from historical analogy, *Trans. Am. Fish. Soc.*, *122*, 647–658.

Nixon, S. W., S. Granger, B. A. Buckley, M. Lamont, and B. Rowell (2004), A one hundred and seventeen year coastal water temperature record from Woods Hole, Massachusetts, *Estuaries*, *27*, 397–404.

Overholtz, W. J., J. A. Hare, and C. M. Keith (2011), Impacts of interannual environmental forcing and climate change on the distribution of Atlantic mackeral on the U.S. Northeast Continental Shelf, *Mar. Coastal Fish. Dyn. Manage. Ecosyst. Sci.*, *3*, 219–232.

Payne, R. E. (1972), Albedo of the sea surface, *J. Atmos. Sci.*, *29*, 959–970.

Ricker, W. E. (1984), Computation and uses of central trend lines, *Can. J. Zool.*, *62*, 1897–1905.

Rosenfeld, L. K. (1983), CODE-1: Moored array and large-scale data report, *Tech. Rep. 83-23*, 186 p., Woods Hole Oceanogr. Inst., Woods Hole, Mass.

Shearman, R. K., and S. J. Lentz (2010), Long-term sea surface temperature variability along the U.S. East Coast, *J. Phys. Oceanogr.*, *40*, 1004–1017.

Smith, S. D. (1988), Coefficients for sea surface wind stress, heat flux, and wind profiles as a function of wind speed and temperature, *J. Geophys. Res.*, *93*(C12), 15,467–15,472.

Taylor, C. C., H. B. Bigelow, and W. H. Graham (1957), Climatic trends and the distribution of marine animals in New England, *Fishery Bull.*, *115*, 293–345.

Thompson, K. R., R. H. Loucks, and R. W. Trites (1988), Sea surface temperature variability in the shelf-slope region of the Northwest Atlantic, *Atmos. Ocean*, *26*, 282–299.

Ullman, D. S., and P. C. Cornillon (2001), Continental shelf surface thermal fronts in winter off the northeast US coast, *Cont. Shelf Res.*, *21*, 1139–1156.

Weinberg, J. R. (2005), Bathymetric shift in the distribution of Atlantic surfclams: Response to warmer ocean temperature, *ICES J. Mar. Sci.*, *62*, 1444–1453, doi:10.1016/j.icesjms.2005.04.020.

Wilkin, J. L. (2006), The summertime heat budget and circulation of southeast New England shelf waters, *J. Phys. Oceanogr.*, *36*, 1997–2011.